Chapter 3

A Survey of Selected Magellanic Cloud Sources

3.1 Introduction

The Magellanic Clouds provide an excellent environment for the study of compact sources, including compact H II regions, supernova remnant candidates, background sources and sources intrinsic to the Clouds. The location of the Clouds away from the Galactic Plane, and the fact that their distances are relatively well-determined, provides a "known" environment in which studies of discrete sources can be undertaken. The Clouds are at a high Galactic latitude where there should be little chance of superposition with foreground sources. Together with the low foreground extinction, this suggests that it should be possible to identify optical counterparts to sources detected at radio frequencies, although in practice this is limited by confusion due to the crowded optical field within the Clouds.

It can be argued that one would expect most compact radio sources in the Magellanic Clouds to be supernova remnants or compact H II regions. SNRs are usually detected at X-ray wavelengths and have a characteristic non-thermal spectrum at centimetre wavelengths. On the other hand, H II regions, with their thermal emission process, are typically weak sources at X-ray wavelengths and have a relatively flat spectrum at centimetre wavelengths. These differences should allow reliable classifications of many of the compact sources in the Clouds. It is also conceivable that a new class of extremely strong compact source might be identified within the Clouds, and that such sources could be used as a probe of the ISM/IGM between the Earth and the Clouds.

The sources chosen for this study were relatively compact at 843 MHz, were a known supernova remnant or a possible SNR candidate, a catalogued H II region or had a possible X-ray detection at or near the position of the radio source. The next three chapters discuss the Magellanic Cloud observing programme to study these compact sources with the ATCA. This chapter presents an overview of the whole programme. A detailed analysis and discussion of the MOST and ATCA observations of the Small

Magellanic Cloud is given in Chapter 4. Analysis and discussion of the Large Magellanic Cloud observations is presented in Chapter 5.

3.2 Choosing the Sources

Choosing a suitable sample often comes down to a compromise between the currently available catalogues and data, the capabilities of the instrument and a realistic expectation of the amount of observing time that can be obtained. An understanding of the capabilities of the instrument is also needed in order to maximize the usefulness of the observing time. For example, a single ATCA observation of a complex source will typically result in a poor quality image due to the insufficient sampling of spatial frequencies. Of course, in addition to instrumental considerations, the astrophysical environment needs to be understood.

3.2.1 Astrophysical Considerations

Sources in both the Small and Large Magellanic Cloud were selected on the basis that they had 843 MHz flux densities greater than 200 mJy and were relatively compact at the angular resolution of the MOST. The astrophysical considerations included:

- such observations would aid in the position calibration of the MOST surveys of the Magellanic Clouds and as a check of the reduction and position-finding software;
- if any of these sources were actually located within the Clouds, they may represent an unusual class of source that could be worthy of further study;
- if a very strong and compact background source was found, it could be used for absorption line studies of the interstellar medium of the Magellanic Clouds.

In addition, the ATCA observations of the SMC targeted a number of sources that met the following criteria:

- Two previously catalogued compact H II regions were chosen because of the presence of adjacent unresolved non-thermal sources at 843 MHz. One of these sources was also coincident with a marginal X-ray detection. Whilst these were likely to be background sources, the non-thermal emission suggested the presence of a supernova remnant.
- Four sources which were marginally detected in the X-ray survey of the SMC by Bruhweiler et al. (1987) were included as there appeared to be associated unresolved MOST sources.
- The known supernova remnant 1E 0102.2-7219 was included. Prior to these observations its radio structure was unknown as it is essentially unresolved at the resolution of the MOST. This source is the subject of a detailed multi-frequency study presented in Chapter 6.

3.2.2 Instrumental Considerations

Preliminary images from the MOST 843 MHz survey of the Magellanic Clouds were available for all the sources discussed in Chapters 4 and 5. Many also appeared in published optical, infrared and X-ray surveys. The MOST data were, at the time, the highest resolution radio observations of the Magellanic Clouds. The instrument capabilities were such that even the preliminary survey images (which had not been deconvolved) provided good sensitivity, particularly to regions of extended emission, allowing the environment surrounding the chosen compact sources to be taken into account when selecting the source list.

In order to observe the chosen number of sources with the ATCA in a reasonable amount of observing time it was decided to observe in a "CUTS" type mode This method, where each source is observed for a short period of time at regular intervals throughout 12–14 hours, is discussed further in the next section.

At the time of these observations, various ATCA systems were still being commissioned, only five of the six antennas were available, no dual frequency/band operation was possible and polarimetry was not supported. The recommended centre frequency in the 6 cm band was 4790 MHz with a nominal continuum bandwidth of 128 MHz.

Follow-up radio observations of some sources were undertaken using the Parkes-Tidbinbilla Interferometer, PTI (Norris et al. 1988), which has since been decommissioned. The PTI provided a real-time, single 275 km baseline interferometer. The correlation was done at the Parkes Observatory and real-time displays gave an indication as to whether a given source was compact and if so, of the approximate flux density. These observations were carried out in the 2.3 GHz band giving an angular resolution of approximately 0.09 arcsec. Only those sources which were compact at the angular scale observed by the ATCA at 5 GHz (based on preliminary reduction of these data) were chosen for followup observations with the PTI. Sources in both the Small and Large Magellanic Clouds were observed.

3.3 Observing and Data Reduction Strategy

When limited to a maximum baseline of 3 km as for the data presented here, the ATCA has an angular resolution of around 3-4 arcsec (HPBW) in the 6 cm band. Observations at a similar frequency undertaken using the Parkes 64 m antenna have an angular resolution of around 5 arcmin. Although there have been a significant number of surveys across a range of centimetre wavelengths, the angular resolution of these was considerably poorer than that offered by the ATCA.

Each source was observed for a short period of time in each "cycle", where a cycle involved observing all the target sources and the phase calibrator(s) and would typically take around an hour. This allowed a reasonable number of sources to be observed, with very good (u, v)-coverage, over a 12-13 hour observing session. Although the integration time using this observing mode for each source is relatively small, the original source selection strategy deliberately chose those sources which were point-like or compact at

the resolution of the MOST. Details of the Small Magellanic Cloud observations are given in Table 3.1 and for the Large Magellanic Cloud observations in Table 3.2.

The advantage of multi-configuration "CUTS" observations can be seen in Figure 3.1 which shows the resulting spatial frequency coverage from all configurations for the observation of the SMC H II region N83/N84. Note that the axes are given in the conventional units of kilo-wavelength (the length of the baseline divided by 1000 $\times$ the wavelength). The figure shows that, although there is reasonably good sampling of a wide range of spatial frequencies, baselines close to zero are not sampled with these configurations. Large scale smooth structure will only be sampled by baselines close to zero. A determination of the integrated flux density of extended sources is likely to be significantly lower than the true value in this case.

Primary flux density calibration was achieved with a single 15 minute observation during each observing session of the standard ATCA primary calibration source B1934–638. Phase calibration for the Small Magellanic Cloud observations was achieved with short observations of two secondary calibrators, B0047–579 and B0252–712, during each cycle. For the Large Magellanic Cloud observations, phase calibration was undertaken using the secondary calibrator B0454–810. These sources were chosen from the standard ATCA calibrator catalogue and have accurate positions determined from VLBI observations. At the time of the observations the hardware necessary for measurement of the phase relationship between the (linear) antenna feeds was not installed, and thus polarimetry was not supported nor attempted.

A number of sources were observed on more than one occasion and in more than one baseline configuration. The reasons for this included:

- Reduction and analysis of the initial observations indicated some interesting structure or feature of the image that required a follow-up observation.
- The source was a known H II region and therefore extended, and thus it was expected that more than a single configuration would be required.
- Instrumental problems sometimes meant that most of the data for a particular observation was seriously affected or unusable. Severe correlator problems occurred on 1990 Dec 16 and the sources affected were re-observed on 1991 Jan 19 and 1991 Apr 24.

Observations undertaken with the ATCA soon after commissioning were limited to a small number of baseline configurations that were denoted simply by sequential numbers (i.e. 1, 2, 3 and 4). Each of these configurations had a maximum baseline length of between 2.5 and 3 km. Based on the observing strategy and results obtained from this and other observing programmes a revised set of baseline configurations was implemented in early 1991. These configurations were labelled to indicate the approximate maximum baseline provided (e.g. #1.5B, #3A). These were better suited to the typical observing programmes that were being undertaken (such as multi-configuration imaging of moderately complex sources).

Table 3.1: Overview of the ATCA 4790 MHz observations of selected sources in the Small Magellanic Cloud. The field centres were selected from preliminary MOST 843 MHz survey images.

Field	Field Centre (B1950.0)	Observation Dates	ATCA Configuration	Approx. Scan Length per "cycle"
BKGS 7	00 51 27 –72 52 20	1990 May 03	1	8 min
BKGS 24	01 15 05 –73 30 30	1990 May 03	1	6 min
BKGS 32	01 19 30 –73 50 10	1990 May 03	1	5 min
BKGS 33	01 24 50 –73 41 20	1990 May 03	1	5 min
N83/N84	01 12 50 –73 34 30	1990 May 03	1	8 min
		1990 Aug 23	2	12 min
		1990 Sep 21	3	10 min
		1990 Dec 16	4	7.5 min
		1991 Jan 19	4	7.5 min
		1991 Apr 24	3A	7.5 min
N90	01 28 55 –73 48 40	1990 May 03	1	8 min
		1990 Aug 23	2	12 min
		1990 Sep 21	3	10 min
		1990 Dec 16	4	7.5 min
		1991 Jan 19	4	7.5 min
		1991 Apr 24	3A	7.5 min
0038–720	00 38 49 –72 02 22	1990 Aug 23	2	5 min
0041–709	00 41 30 –70 58 10	1990 Aug 23	2	5 min
		1990 Dec 16	4	4 min
		1991 Jan 19	4	4 min
		1991 Apr 24	3A	4 min
0054–713	00 54 24 –71 23 18	1990 Aug 23	2	5 min
0055–744	00 55 57 –72 28 54	1990 Aug 23	2	5 min
0109–735	01 09 24 –73 30 20	1990 Aug 23	2	5 min
		1990 Dec 16	4	4 min
		1991 Jan 19	4	4 min
		1991 Apr 24	3A	4 min
0021–742	00 21 40 –74 13 00	1990 Dec 16	4	4 min
		1991 Jan 19	4	4 min
		1991 Apr 24	3A	4 min
0032–738	00 32 40 –73 51 00	1990 Dec 16	4	4 min
		1991 Jan 19	4	4 min
		1991 Apr 24	3A	4 min
0036–746	00 36 50 –74 38 00	1990 Dec 16	4	4 min
		1991 Jan 19	4	4 min
		1991 Apr 24	3A	4 min
0037–719	00 37 45 –71 54 30	1990 Dec 16	4	4 min
		1991 Jan 19	4	4 min
		1991 Apr 24	3A	4 min
0050–727	00 50 16 –72 43 00	1990 Dec 16	4	4 min
		1991 Jan 19	4	4 min
		1991 Apr 24	3A	4 min
0058–719	00 58 45 –71 52 30	1990 Dec 16	4	4 min
		1991 Jan 19	4	4 min
		1991 Apr 24	3A	4 min
0107–718	01 08 10 –71 51 30	1990 Dec 16	4	4 min
		1991 Jan 19	4	4 min
		1991 Apr 24	3A	4 min
0109–727	01 08 45 –72 44 00	1990 Dec 16	4	4 min
		1991 Jan 19	4	4 min
		1991 Apr 24	3A	4 min
0131–729	01 31 30 –72 55 00	1990 Dec 16	4	4 min
		1991 Jan 19	4	4 min
		1991 Apr 24	3A	4 min

Table 3.2: Overview of the ATCA 4790 MHz observations of selected sources in the Large Magellanic Cloud. The field centres were selected from preliminary MOST 843 MHz survey images.

Field	Field Centre (B1950.0)	Observation Dates	ATCA Configuration	Approx. Scan Length per "cycle"
0458–720	04 58 50 –72 01 00	1990 Dec 20	4	4 min
		1991 Jan 21	4	4 min
0502–696	05 02 40 –69 36 00	1990 Dec 20	4	4 min
		1991 Jan 21	4	4 min
0505–681	05 05 27 –68 07 00	1990 Dec 20	4	4 min
		1991 Jan 21	4	4 min
0510–689	05 10 00 –68 57 00	1990 Dec 20	4	4 min
		1991 Jan 21	4	4 min
0512–671	05 12 30 –67 11 00	1990 Dec 20	4	4 min
		1991 Jan 21	4	4 min
0513–692	05 13 30 –69 15 00	1990 Dec 20	4	6 min
		1991 Jan 21	4	6 min
0515–674	05 15 40 –67 24 00	1990 Dec 20	4	4 min
		1991 Jan 21	4	4 min
0518–696	05 19 20 –69 41 00	1990 Dec 20	4	4 min
		1991 Jan 21	4	4 min
0524–708	05 24 15 –70 54 00	1990 Dec 20	4	4 min
		1991 Jan 21	4	4 min
0528–692	05 28 00 –69 14 00	1990 Dec 20	4	6 min
		1991 Jan 21	4	6 min
0532–675	05 32 30 –67 34 00	1990 Dec 20	4	4 min
		1991 Jan 21	4	6 min
0534–720	05 35 00 –72 04 00	1990 Dec 20	4	4 min
		1991 Jan 21	4	6 min
0547–677	05 48 00 –67 47 00	1990 Dec 20	4	4 min
		1991 Jan 21	4	6 min
0550–684	05 50 40 –68 24 00	1990 Dec 20	4	4 min
		1991 Jan 21	4	6 min
0440–665	04 40 50 –66 30 00	1991 Jan 18	4	4 min
0449–709	04 49 30 –70 57 00	1991 Jan 18	4	4 min
0454–649	04 54 44 –64 55 00	1991 Jan 18	4	4 min
0515–660	05 15 20 –66 02 00	1991 Jan 18	4	4 min
0517–718	05 17 30 –71 52 00	1991 Jan 18	4	4 min
0526–659	05 26 20 –65 59 00	1991 Jan 18	4	4 min
0526–658	05 26 20 –65 50 20	1991 Jan 18	4	4 min
0527–651	05 28 00 –65 06 00	1991 Jan 18	4	4 min
0533–725	05 33 50 –72 34 00	1991 Jan 18	4	4 min
0537–692	05 36 50 –69 18 00	1991 Jan 18	4	4 min
0540–696	05 40 30 –69 40 00	1991 Jan 18	4	4 min
0545–649	05 45 40 –64 55 00	1991 Jan 18	4	4 min
0552–703	05 52 55 –70 22 30	1991 Jan 18	4	4 min
0600–706	06 00 45 –70 38 00	1991 Jan 18	4	4 min
0451–696	04 51 50 –69 38 30	1991 Jan 19	4	4 min
		1991 Apr 24	3A	4 min
0456–703	04 56 40 –70 19 00	1991 Jan 19	4	4 min
		1991 Apr 24	3A	4 min
0503–680	05 02 50 –68 02 00	1991 Jan 19	4	4 min
		1991 Apr 24	3A	4 min
0504–668	05 05 10 –66 47 30	1991 Jan 19	4	4 min
		1991 Apr 24	3A	4 min
0514–676	05 14 20 –67 39 00	1991 Jan 19	4	4 min
		1991 Apr 24	3A	4 min
0518–679	05 18 00 –67 59 00	1991 Jan 19	4	4 min
		1991 Apr 24	3A	4 min
0530–678	05 30 00 –67 51 00	1991 Jan 19	4	4 min
		1991 Apr 24	3A	4 min
0535–676	05 35 45 –67 36 00	1991 Jan 19	4	4 min
		1991 Apr 24	3A	4 min
0541–670	05 41 40 –67 00 00	1991 Jan 19	4	4 min
		1991 Apr 24	3A	4 min
0543–681	05 43 15 –68 08 40	1991 Jan 19	4	4 min
		1991 Apr 24	3A	4 min
0543–710	05 43 30 –71 04 00	1991 Jan 19	4	4 min
		1991 Apr 24	3A	4 min
0545–719	05 45 20 –71 56 00	1991 Jan 19	4	4 min
		1991 Apr 24	3A	4 min
0547–704	05 47 00 –70 27 30	1991 Jan 19	4	4 min
		1991 Apr 24	3A	4 min
0552–682	05 52 20 –68 15 00	1991 Jan 19	4	4 min
		1991 Apr 24	3A	4 min

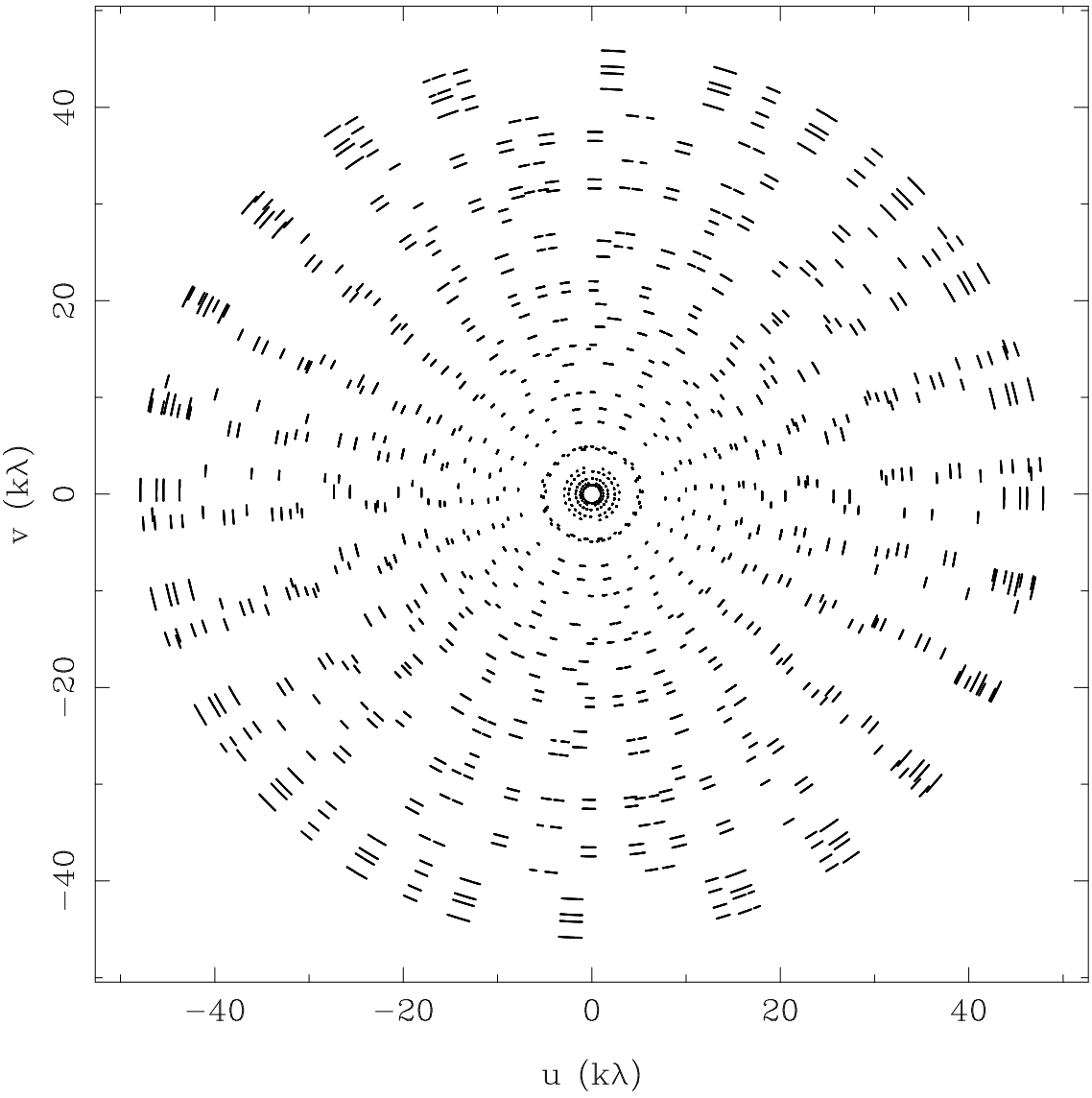

Figure 3.1: The spatial frequency coverage of the multi-configuration ATCA 4790 MHz total intensity observation of SMC N83/N84.

Although the observed field centres are given in equinox and epoch B1950.0 the ATCA online observing software converts these to J2000.0 and the data are recorded in J2000.0 coordinates. All subsequent analysis has been done in J2000.0 coordinates and all images are presented in equinox and epoch of J2000.0. Much of the published catalogue data is given in B1950.0 coordinates. When required, these were precessed using standard available packages, to J2000.0 for comparison with the data reported here. All astronomical coordinates are expressed with right ascension in hh mm ss and declination in dd mm ss.

3.3.1 Data Reduction

As these data were obtained early in the life of the instrument, careful data editing was needed in order to produce images of acceptable quality. In some cases entire scans had to be deleted or particular antenna and baseline combinations completely flagged as a result of significant correlator and/or data transfer problems.

Soon after the observations were completed a preliminary reduction of the data was made entirely within the Astronomical Image Processing System ($\mathcal{AIPS}$) which, at the time, was the recommended (and documented) method for reducing ATCA data. The data are loaded using a special local task `ATLOD` and then the standard reduction tasks used to edit, calibrate, image, deconvolve and display the data.

Data obtained over a number of observing sessions and in various baseline configurations were combined into a single multi-configuration UV dataset again using standard procedures within $\mathcal{AIPS}$. This combined and calibrated dataset was used for imaging and subsequent analysis. Although all analysis could have been done in $\mathcal{AIPS}$, the $\mathcal{MIRIAD}$ package (Sault et al. 1995) was used for the final data editing, imaging, deconvolution, display and analysis. This decision was taken because $\mathcal{MIRIAD}$ is better suited to modern workstation and display environments and because its design is more flexible than $\mathcal{AIPS}$. It is also far simpler to make minor modifications to existing tasks if desired. Both $\mathcal{AIPS}$ and $\mathcal{MIRIAD}$ have their own on-disk data format so the only viable method for transferring the data between packages is via FITS. Although a somewhat tedious process no problems were experienced in the transfer of the edited and calibrated visibility data between the software packages.

Each UV dataset was inspected with the $\mathcal{MIRIAD}$ task `uvplt` (typically using per-baseline plots of amplitude versus hour angle) and further editing, if needed, carried out with `uvflag`. Bad data were excised by the bulk deletion of all visibilities typically above a certain flux density for a given set of baselines. Stokes Q, U and V were flagged in addition to Stokes I for completeness.

Each field was imaged using `invert` with a pixel spacing of 0.5 arcsec, which gives adequate sampling of the beam, and an image size of 1024×1024 pixels. The image quality was assessed and, if necessary, further editing undertaken. Once the image was deemed to be acceptable, a simple deconvolution was done using `clean` with a limit of 100 components and the (default) loop gain of 0.1. Given the expected source morphology, this form of deconvolution was adequate. The final image was produced using `restor`. Subimages of the more interesting regions were made using `imsub` and

are typically of size 64×64 pixels with the source of interest at or very near to the centre of the subimage. These subimages were used for the subsequent analysis and are shown in Chapters 4 and 5.

The *MIRIAD* task `imsad` was used to obtain the source parameters of those sources which were compact at 4790 MHz. This task fits a single gaussian component to an "island" of pixels which are contiguous and lie above some cutoff. To determine the true image RMS noise, the task fits a gaussian to a histogram of the image. For these data, the cutoff level for "island" detection was usually set to be three times the RMS noise as determined from the image histogram, although for some of the stronger LMC sources this was set to five times the RMS noise.

The resulting parameters include the position of centroid (which is not necessarily at the same position as the pixel with maximum intensity), the peak and integrated flux densities and the deconvolved source axes (FWHM) and position angle. In addition, a number of flags are output to indicate the success or otherwise of the fitting procedure.

3.3.2 Derived Parameters and Source Classification

A number of parameters can be derived from the ATCA data for comparison with data from other surveys and catalogues. These include:

- *Source position.* Needed for accurate comparison to published catalogues and for reference to the MOST survey positions.

- *Source morphology.* As these images have an angular resolution of around 4 arcsec, some sources which appear compact in lower-resolution images are revealed to have a complex and interesting morphology. Such information can aid in the determination of their nature by comparison with published results.

- *Peak and integrated flux density.* These were obtained directly from the fitting procedure in most cases. In some cases, if the source was significantly extended, different procedures had to be adopted. Where this was necessary, it is mentioned in the discussion for that particular source.

Comparing the ATCA positions to existing catalogues requires care as the previous radio surveys undertaken using the Parkes 64 m antenna have an effective beam size (HPBW) of around 5 arcmin, much larger than that of the ATCA. In addition, these "single-dish" Parkes observations at centimetre wavelengths will be sensitive to extended thermal emission (such as that from H II regions) which is abundant in the Clouds. Thus there is some uncertainty in making a direct comparison between the high resolution ATCA data and the lower angular resolution data in published catalogues. A more direct comparison can be made between the interferometric ATCA data and MOST data, as the latter have a resolution of around 43 arcsec (HPBW).

To be able to classify sources with any degree of certainty, at least the following criteria need to be taken into account:

- The morphology and extension of the source at various frequencies.
- Optical and infrared emission. Obtaining optical identifications in a region such as the Magellanic Clouds is difficult and is likely to only be possible for those sources which are located in relatively isolated regions. Infrared emission can be used to aid in the confirmation that thermal emission processes are occurring such as would be observed from an H II region.
- Presence of X-ray emission. The presence of X-ray emission indicates that non-thermal emission processes are occurring. This, taken alongside morphology considerations and the source spectrum, would provide relatively strong evidence that the source could be, for example, a supernova remnant.
- Spectral index. As this is derived from the integrated flux density there is a reasonable possibility that the calculated value would have a significant uncertainty. Thus, although a useful parameter, the spectral index needs to be used with caution. Many issues associated with the determination of spectral indices are discussed in detail in Chapter 4, and are revisited in Chapter 5 in which a systematic method of classifying sources (termed a "decision tree") is introduced.
- H I distance. If a source was particularly strong, then it may be possible to undertake H I spectral line observations to determine its location relative to the Magellanic Clouds along the line-of-sight from the Earth. This is likely to be possible only for a small number of sources.

Using these criteria along with published data across of range of wavelengths, it should be possible to classify the sources into the following broad categories:

- Background sources. Often these will be compact and have a relatively steep spectrum. The determination of the H I distance could be used to confirm that the object is behind the Clouds but most sources will not have sufficient intensity for spectral line observations.
- Supernova remnant or supernova remnant candidate. Morphology, spectrum and the presence of X-ray emission are typically the important criteria to consider in order to classify a source as a SNR or SNR candidate.
- H II regions. Typically these regions have a relatively flat spectrum and associated Hα emission. In most, if not all cases, the region will be listed in the published catalogues.

3.3.3 Radio Source Counts

As well as classifying individual sources using the criteria discussed above, it is also useful to calculate the expected number of sources for a given area of sky. This is usually referred to as the $\log N/\log S$ curve. Following the treatment given by Large

(1990) a brief outline of how radio source counts are derived and the assumptions made in determining the source count is as follows.

For a static, Euclidean, isotropic universe which is populated by identical non-evolving radio sources, the distribution of radio sources as a function of flux density S, may be represented by the function:

$$N_0(\geq S) = N_1 \, (S/S_1)^{-1.5}, \tag{3.1}$$

where N_0 is the number of sources per steradian observed with a flux density $\geq S$ and N_1 and S_1 are constants.

It is widely accepted that source counts are expressed in terms of a model Euclidean universe and standard observing frequency, in which the constants N_1 and S_1 are $100\,\mathrm{sr}^{-1}$ and 1 Jy respectively (see, for example, Wall & Peacock 1985). Thus, Equation 3.1 becomes:

$$N_0 = 100\, S^{-1.5} \tag{3.2}$$

which is the *integral source count* for the model Euclidean universe. The differential form of Equation 3.2 (ignoring signs) thus becomes:

$$dN_0/dS = 150\, S^{-2.5} \tag{3.3}$$

which gives the number of radio sources per flux density range for the same model and is referred to as the *differential source count*. Observed source counts then differ from Equation 3.3 by a factor which depends on the observing frequency and the flux density as follows:

$$dN/dN_0 = f(S, \nu). \tag{3.4}$$

Commonly, $f(S, \nu)$ is referred to as (n/n_0) which expresses the departure of the observed universe from the Euclidean model, the specific observing frequency, and the difference between the real source population and a uniform non-evolving source population in a Euclidean geometry. Equation 3.3 then becomes:

$$dN/dS = 150\, (n/n_0)\, S^{-2.5}. \tag{3.5}$$

Radio source counts are usually presented as a graph of (n/n_0) against S for a given frequency.

Equation 3.5 can be integrated over a given flux density range to determine the number of sources per steradian giving:

$$N(S_1 \leq S < S_2) = \int_{S_1}^{S_2} 150 \left(\frac{n}{n_0}\right) S^{-2.5} \, dS. \tag{3.6}$$

For MOST 843 MHz data, Large (1990) determined (n/n_0), with an uncertainty of around 10%, by fitting lines to source count data in three distinct flux density ranges ($S < 0.2\,\mathrm{Jy}$, $0.2\,\mathrm{Jy} \leq S < 2\,\mathrm{Jy}$ and $S \geq 2\,\mathrm{Jy}$). Thus, from Equation 3.6 the radio source counts per square degree can be calculated for a given flux density range.

3.4 Summary

This chapter presents an overview of the MOST and ATCA observations of the Small and Large Magellanic Clouds, along with details of the observing methodology, astrophysical considerations and analysis techniques used in this study. The importance of a thorough understanding of the instrumentation and related issues in order to conduct a successful survey of compact sources using a small number of interferometer baselines in a limited amount of observing time has been highlighted.

A discussion of the parameters which can be determined from these observations has been presented along with a overview of a number of factors that need to be considered to permit the correct classification of a given source.